Supplement of Atmos. Chem. Phys., 15, 1683–1705, 2015
http://www.atmos-chem-phys.net/15/1683/2015/
doi:10.5194/acp-15-1683-2015-supplement

Atmospheric Chemistry and Physics Open Access

Supplement of

Source sector and region contributions to BC and $PM_{2.5}$ in Central Asia

S. Kulkarni et al.

Correspondence to: N. Sobhani (negin-sobhani@uiowa.edu) and G. R. Carmichael (gcarmich@engineering.uiowa.edu)

To study the regional differences in MODIS and modeled AOD over the domain of interest in this study, the regional average AOD values on a daily scale were extracted from MODIS and model over the specific regions defined in Fig. 1 of main manuscript including CA, Middle East, South Asia, Europe, China and Russia. The period mean MODIS AOD over the selected regions is shown Fig. S5 and Table S2 with a mean value of ~ 0.3 ranging from ~0.15 in Europe to 0.44 over South Asia, while the simulated AOD average is ~ 0.28 with the minimum value of ~0.19 and ~0.32 seen over Europe and South Asia respectively. Negative biases are seen over South Asia, Central Asia and Middle East, while positive biases are seen over Europe, Russia and China suggesting that the simulated values are underpredicted and overpredicted respectively in these regions. These regional average biases are in general consistent with the variability and spatial patterns seen in Fig.3b of main manuscript.

The seasonality in average MODIS and modeled AOD values is shown as monthly box plots for the selected source regions over the simulation time period in Fig S6. (The seasonal spatial plots are presented in Fig. S11). It can be seen that the regional average MODIS AOD captures the general seasonality seen in AOD values with high values in spring/summer associated with dust enhancements and buildup of anthropogenic pollutants in all regions. The predicted AOD shows a similar seasonal cycle with a tendency to over-predict AOD over Russia (Fig. S6f), Europe (Fig. S6c), China (Fig. S6d) during the winter months. . The modeled values show a systematic underprediction in AOD over South Asia (Fig. S6e) and Middle East (Fig.S6b) regions during all seasons. The simulated Central Asia average AOD (Fig. S6a) shows a large underprediction in the months of July through September but overpredicts in the months of February through May 2009.

The comparison of MODIS and modeled AOD over the specific regions and the associated seasonality described above shows that the simulated AOD is able to capture the general features of regional distribution and seasonal cycle seen in observed MODIS values.

Table S1. List of Sites from AERONET, EANET and EMEP used in this study (See Sect. 3.2 for details)

AERONET Site Locations

Site	Latitude	Longitude	Site	Latitude	Longitude	Site	Latitude	Longitude
Abu_Al_Bukhoosh	25.50	53.15	Caceres	39.48	-6.34	Gandhi_College	25.87	84.13
Arcachon	44.66	-1.16	Carpentras	44.08	5.06	Gosan_SNU	33.29	126.16
ATHENS-NOA	37.99	23.78	Chen-Kung_Univ	23.00	120.22	Graciosa	39.09	-28.03
Autilla	42.00	-4.60	Chilbolton	51.14	-1.44	Granada	37.16	-3.61
Avignon	43.93	4.88	Creteil	48.79	2.44	Gual_Pahari	28.43	77.15
Bac_Giang	21.29	106.23	Dalanzadgad	43.58	104.42	Gustav_Dalen_Tower	58.59	17.47
Baneasa	44.51	26.08	Davos	46.81	9.84	Gwangju_GIST	35.23	126.84
Barcelona	41.39	2.12	Dhabi	24.48	54.38	Hamburg	53.57	9.97
Bareilly	28.39	79.44	Dhadnah	25.51	56.32	Hefei	31.90	117.16
Beijing	39.98	116.38	Dongsha_Island	20.70	116.73	Helgoland	54.18	7.89
Belsk	51.84	20.79	Dunkerque	51.04	2.37	Helsinki	60.20	24.96
Birkenes	58.39	8.25	Eforie	44.08	28.63	Helsinki_Lighthouse	59.95	24.93
Blida	36.51	2.88	Eilat	29.50	34.92	Hetauda	27.43	85.03
Brussels	50.78	4.35	El_Arenosillo	37.11	-6.73	Hong_Kong_Hok_Tsui	22.21	114.26
Bucharest_Inoe	44.35	26.03	EPA-NCU	24.97	121.19	Hong_Kong_PolyU	22.30	114.18
Burjassot	39.51	-0.42	Ersa	43.00	9.36	Hyytiala	61.85	24.30
Burjassot	39.51	-0.42	EVK2-CNR	27.96	86.81	IASBS	36.71	48.51
Cabauw	51.97	4.93	Evora	38.57	-7.91	IFT-Leipzig	51.35	12.44
Cabo_da_Roca	38.78	-9.50	Fontainebleau	48.41	2.68	IIT_KGP_EXT_Kolkata	22.57	88.42
Cabo_Raso	38.71	-9.49	FORTH_CRETE	35.33	25.28	IMAA_Potenza	40.60	15.72

Table S1. (Continued) List of Sites from AERONET, EANET and EMEP used in this study (See Sect. 3.2 for details)

AERONET Site Locations								
Site	Latitude	Longitude	Site	Latitude	Longitude	Site	Latitude	Longitude
IMS-METU-ERDEMLI	36.57	34.26	Lahore	31.54	74.32	NCU_Taiwan	24.97	121.19
Irkutsk	51.80	103.09	Langtang	28.01	85.49	Nes_Ziona	31.92	34.79
Ispra	45.80	8.63	Lanzhou_City	36.05	103.85	New_Delhi	28.63	77.18
Issyk-Kul	42.62	76.98	Le_Fauga	43.38	1.28	OHP_OBSERVATOIRE	43.94	5.71
Izana	28.31	-16.50	Lecce_University	40.34	18.11	Oostende	51.23	2.93
Jaipur	26.91	75.81	Lille	50.61	3.14	Oukaimeden	31.21	-7.88
Jingtai	37.33	104.10	London-UCL-UAO	51.52	-0.13	Palaiseau	48.70	2.21
Kaiping	22.32	112.54	Lulin	23.47	120.87	Palencia	41.99	-4.52
Kandahar	31.51	65.85	Mainz	50.00	8.30	Palgrunden	58.76	13.15
Kanpur	26.51	80.23	Malaga	36.72	-4.48	Pantnagar	29.05	79.52
Kanzelhohe_Obs	46.68	13.91	Messina	38.20	15.57	Paris	48.87	2.33
Karachi	24.87	67.03	Mezaira	23.15	53.78	PKU_PEK	39.59	116.18
Karlsruhe	49.09	8.43	Minsk	53.92	27.60	Rome_Tor_Vergata	41.84	12.65
Kathmandu_Univ	27.60	85.54	Modena	44.63	10.95	Saada	31.63	-8.16
Kuopio	62.89	27.63	Moldova	47.00	28.82	Saint_Mandrier	43.07	5.94
Kuwait_Airport	29.24	47.97	Moscow_MSU_MO	55.70	37.51	Salon_de_Provence	43.61	5.12
Kuwait_University	29.33	47.97	Munich_University	48.15	11.57	Santa_Cruz_Tenerife	28.47	-16.25
Kyiv	50.36	30.50	Mussafa	24.37	54.47	SEDE_BOKER	30.86	34.78
La_Laguna	28.48	-16.32	Nainital	29.36	79.46	Sevastopol	44.62	33.52
Laegeren	47.48	8.35	NAM_CO	30.77	90.96	Seysses	43.50	1.26

Table S1. (Continued) List of Sites from AERONET, EANET and EMEP used in this study (See Sect. 3.2 for details)

Aeronet Sites			EANET sites			EMEP sites		
Site	Latitude	Longitude	Site	Latitude	Longitude	Site	Latitude	Longitude
Shouxian	32.56	116.78	Bangkok	13.77	100.53	Aspvreten	58.80	17.38
Solar_Village	24.91	46.40	Banryu	34.68	131.80	Braganca	41.82	-6.77
Taihu	31.42	120.22	Cheju	33.30	126.17	CEHedinburgh	55.95	-3.22
Taipei_CWB	25.03	121.50	ChiangMai	18.77	98.93	Illmitz	47.77	16.77
Tamanrasset_INM	22.79	5.53	Happo	36.70	137.80	Ispra	45.80	8.63
Thessaloniki	40.63	22.96	Hedo	26.87	128.25	Kollumerwaard	53.33	6.28
Tomsk	56.48	85.05	Hongwen	24.47	118.13	Kosetice	49.58	15.08
Toravere	58.26	26.46	Ijira	35.57	136.68	MaceHead	53.17	-9.50
Toulon	43.14	6.01	Imsil	35.60	127.18	UniversityofGent	51.05	3.72
Tremiti	42.12	15.49	Jinyunshan	29.82	106.37	VirolahtII	60.53	27.69
TUBITAK_UZAY_Ankara	39.89	32.78	Kanghwa	37.70	126.28	Waldhof	52.80	10.76
Tuz_Golu	38.75	33.34	Ochiisi	43.15	145.50			
Venise	45.31	12.51	Ogasawara	27.08	142.22			
Villefranche	43.68	7.33	Oki	36.28	133.18			
Wytham_Woods	51.77	-1.33	Rishiri	45.12	141.20			
Xanthi	41.15	24.92	SadoSeki	38.33	138.40			
XiangHe	39.75	116.96	Samutprakarn	13.73	100.57			
Xinglong	40.40	117.58	Tappi	41.25	140.35			
Yakutsk	61.66	129.37	Xiang_Zhou	22.27	113.57			
Yekaterinburg	57.04	59.55	Yusuhara	33.37	132.93			
Zhangye	39.08	100.28						
Zvenigorod	55.70	36.78						

Table S2. Statistical summary of comparison of regional average MODIS and modeled AOD over selected source regions including CA, China, Europe, Middle East, Russia and South Asia . (See Fig 1 and Sect.3.2 for more details)

Parameter	**C. Asia**	**China**	**Europe**	**Middle East**	**Russia**	**South Asia**	**All**
Number of data points	458	459	459	459	453	459	2747
Mean obs	0.31	0.36	0.15	0.36	0.19	0.44	0.30
Mean model	0.28	0.36	0.19	0.29	0.25	0.32	0.28
Standard deviation obs	0.09	0.15	0.05	0.14	0.10	0.16	0.16
Standard deviation model	0.09	0.10	0.06	0.12	0.10	0.14	0.12
Mean Bias	-0.03	0.00	0.04	-0.07	0.05	-0.13	-0.02
Mean Error	0.08	0.07	0.06	0.08	0.08	0.14	0.08
Root mean sqauared error	0.10	0.10	0.07	0.10	0.11	0.17	0.11
Fractional Mean Bias (%)	-9.16	4.57	24.05	-21.37	26.18	-34.26	-1.72
Fractional Mean Error (%)	26.06	21.21	33.45	24.96	36.02	37.22	29.81
Mean Normalized Bias (%)	-3.96	8.56	36.47	-17.60	46.82	-26.64	7.19
Mean Normalized Error (%)	25.37	23.17	44.85	21.73	55.43	30.02	33.38
Normalized Mean Bias (%)	-9.54	0.30	26.39	-19.57	26.20	-28.22	-7.38
Normalized Mean Error (%)	24.92	20.55	37.24	22.22	40.25	30.72	27.60
R-squared	0.18	0.60	0.19	0.74	0.28	0.56	0.52

Table S3. Statistical summary of comparison of observed and modeled surface meteorological parameters at the a) LST and b) Bishkek sites.

(a) Site : LST	T(K)		RH%		WS(m/s)		WDir	
	Obs	MDL	Obs	MDL	Obs	MDL	Obs	MDL
Mean	280.3	27.2	59.2	61.7	3.0	4.5	182.1	220.8
Standard Error	0.4	0.4	0.8	0.8	0.0	0.1	1.3	2.9
Median	280.9	279.4	58.3	60.0	3.0	4.0	183.3	235.0
Standard Deviation	7.9	8.2	15.4	16.3	0.7	1.7	26.3	57.2
Sample Variance	61.7	67.2	236.1	265.1	0.5	3.0	691.4	3276.1
Range	30.7	34.5	71.2	73.6	4.4	11.1	149.3	293.7
Minimum	266.1	260.6	26.8	20.1	0.7	1.6	109.3	31.4
Maximum	296.8	295.1	97.9	93.7	5.2	12.7	258.6	325.1
Count	382.0	382.0	382.0	382.0	382.0	382.0	382.0	382.0
Confidence Level (95.0%)	0.8	0.8	1.5	1.6	0.1	0.2	2.6	5.8
RMSE	2.4		13.2		2.5		131.3	
Mean Bias Error	-1.2		2.4		1.5		86.2	
Mean Normalized Bias Error	0.0		0.1		0.7		0.5	
Pearson's R	1.0		0.7		-0.1		0.1	
R-squared	0.9		0.4		0.0		0.0	

(b) Site: Bishkek	T(K)		RH (%)		WS(m/s)		WDir	
	Obs	MDL	Obs	MDL	Obs	MDL	Obs	MDL
Mean	288.0	287.9	51.8	46.4	0.7	4.1	216.0	180.3
Standard Error	0.5	0.4	1.0	0.7	0.0	0.1	2.1	2.8
Median	288.9	289.1	50.2	43.1	0.7	3.9	221.5	201.3
Standard Deviation	10.1	9.2	21.1	15.4	0.3	1.2	46.8	62.5
Sample Variance	102.5	85.6	443.8	236.6	0.1	1.4	2189.1	3912.0
Range	40.0	37.3	80.8	71.7	2.3	7.4	298.3	239.0
Minimum	266.3	267.2	16.5	20.7	0.4	1.6	61.7	55.8
Maximum	306.3	304.4	97.3	92.4	2.8	9.0	360.0	294.8
Count	486.0	486.0	484.0	484.0	483.0	483.0	484.0	484.0
Confidence Level (95.0%)	0.9	0.8	1.9	1.4	0.0	0.1	4.2	5.6
RMSE	3.1		13.5		3.5		86.2	
Mean Bias Error	-0.2		-5.4		3.3		-35.7	
Mean Normalized Bias Error	0.0		0.0		5.1		0.1	
Pearson's R	1.0		0.8		0.1		0.0	
R-squared	0.9		0.7		0.0		0.0	

Table S4. Statistical summary of comparison of observed and modeled surface AOD and PM at a) LST and b) Bishkek sites.

(a) Site : LST	AOD				$PM_{2.5}(\mu g/m^3)$			$PM_{10}(\mu g/m^3)$		OC(µg /m3)		BC(µg /m3)	
	Obs-SP	MDL	Obs-LE	MDL[1]	Filter	TEOM-NonVOL	MDL	Filter	MDL	Filter	MDL	Filter	MDL
Mean	0.19	0.25	0.28	0.28	7.21	6.98	11.31	15.82	29.59	1.48	0.23	0.29	0.11
Standard Error	0.01	0.01	0.02	0.01	0.35	0.34	0.55	1.06	2.04	0.09	0.01	0.02	0.00
Median	0.15	0.24	0.16	0.24	5.80	5.99	10.01	12.04	20.76	1.16	0.19	0.20	0.10
Standard Deviation	0.14	0.12	0.26	0.17	4.31	4.09	6.74	14.31	27.45	1.17	0.16	0.26	0.04
Sample Variance	0.02	0.01	0.07	0.03	18.57	16.72	45.46	204.86	753.33	1.36	0.03	0.07	0.00
Range	0.85	1.00	1.29	1.17	25.77	22.26	57.15	130.39	200.86	9.71	1.26	1.50	0.42
Minimum	0.04	0.08	0.03	0.07	1.00	0.93	3.53	1.69	6.83	0.04	0.07	0.00	0.04
Maximum	0.89	1.08	1.33	1.25	26.77	23.19	60.69	132.08	207.69	9.75	1.33	1.50	0.46
Count	286	286	171	171	148	148	148	181	181	179	179	179	179
Confidence Level (95.0%)	0.02	0.01	0.04	0.03	0.70	0.66	1.10	2.10	4.03	0.17	0.02	0.04	0.01
RMSE	0.16		0.28		7.86	7.84		28.93		1.72		0.32	
Mean Bias Error	0.06		0.00		4.10	4.32		13.77		-1.26		-0.19	
Mean Normalized Bias Error	0.83		0.93		1.04	1.03		1.68		-0.73		-0.14	
Pearson's R	0.34		0.23		0.32	0.35		0.39		0.02		0.22	
R-squared	0.12		0.05		0.10	0.12		0.15		0.00		0.05	

[1-] These model results are for the comparison with the LE observations.

(b) Site: Bishkek	AOD		$PM_{2.5}$(µg/m^3)		PM_{10}(µg/m^3)		OC (µg/m^3)		BC(µg/m^3)	
	Obs(SP)	MDL	Filter	MDL	Obs	MDL	Obs	MDL	Obs	MDL
Mean	0.21	0.25	8.65	11.87	17.66	29.79	1.49	0.21	0.27	0.10
Standard Error	0.01	0.01	0.38	0.61	0.94	2.02	0.07	0.01	0.02	0.00
Median	0.17	0.24	7.95	9.65	14.01	21.83	1.46	0.18	0.23	0.10
Standard Deviation	0.15	0.12	5.23	8.26	12.80	27.51	0.93	0.13	0.20	0.04
Sample Variance	0.02	0.01	27.39	68.18	163.72	756.74	0.87	0.02	0.04	0.00
Range	0.87	0.89	29.91	59.45	77.00	191.20	5.26	1.19	1.30	0.40
Minimum	0.03	0.08	0.53	2.32	0.87	5.74	-0.03	0.07	0.01	0.04
Maximum	0.90	0.98	30.44	61.77	77.87	196.94	5.23	1.26	1.31	0.43
Count	341	341	186	186	186	186	186	186	170	170
Confidence Level (95.0%)	0.02	0.01	0.76	1.19	1.85	3.98	0.13	0.02	0.03	0.01
RMSE	0.18		9.76		30.77		1.57		0.26	
Mean Bias Error	0.04		3.22		12.13		-1.28		-0.17	
Mean Normalized Bias Error	0.79		1.33		2.34		-0.72		-0.18	
Pearson's R	0.19		0.12		0.39		0.22		0.17	
R-squared	0.04		0.01		0.15		0.05		0.03	

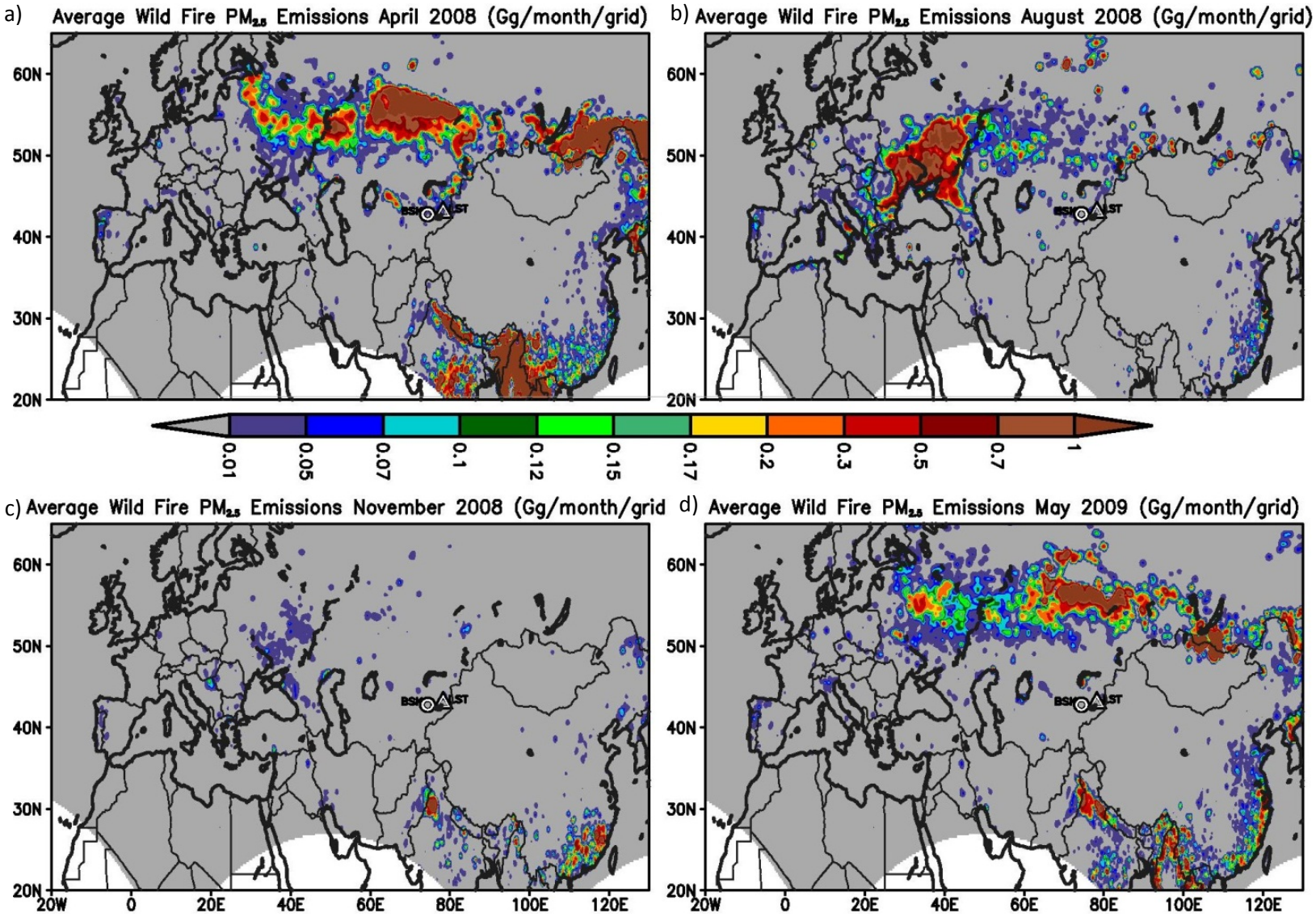

Fig. S1. Seasonal variability in spatial distribution of biomass burning $PM_{2.5}$ emissions in Gg/month/grid (a) April 2008, (b) August 2008, (c) November 2008, and (d) May 2009.

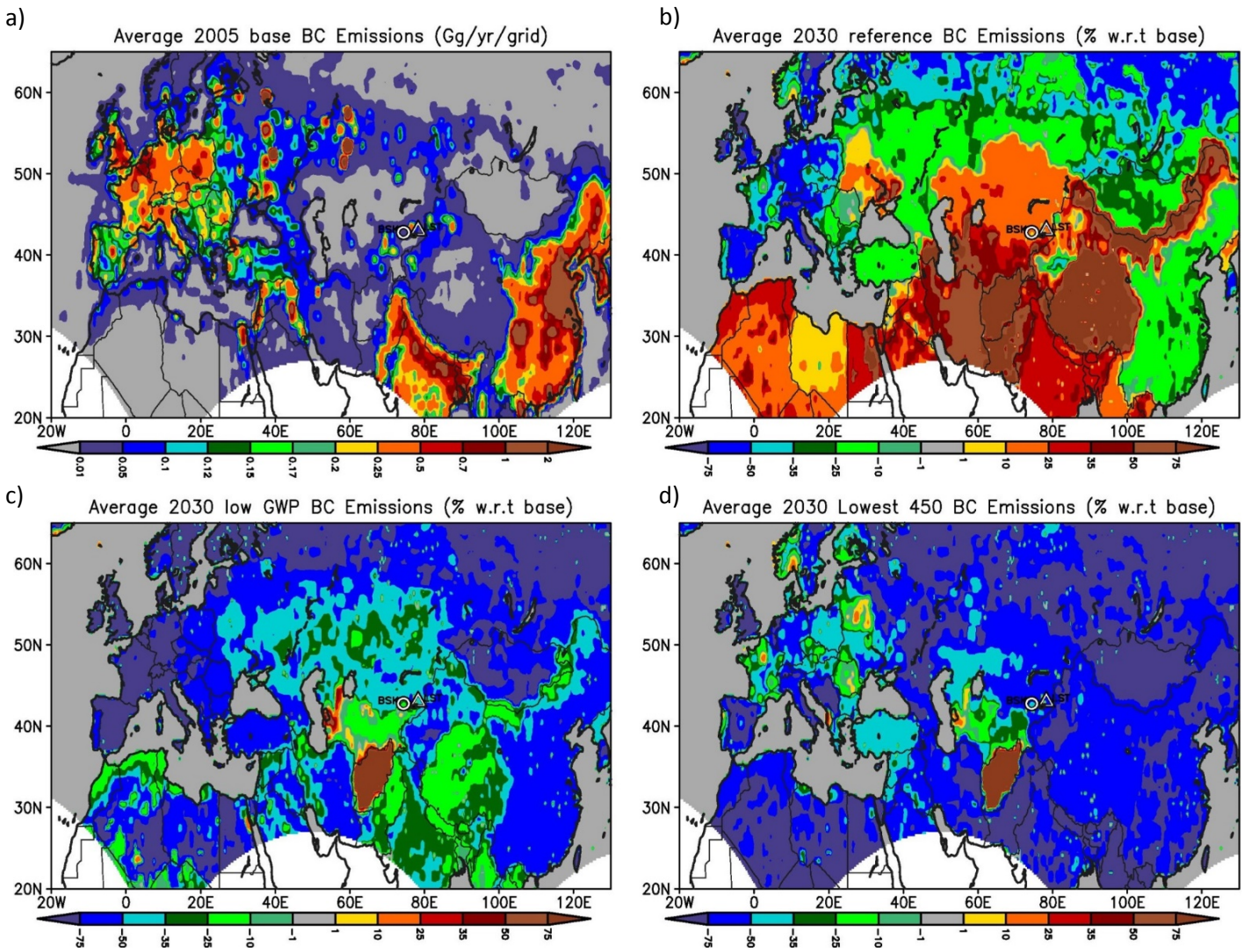

Fig. S2. Spatial distribution of a) base year 2005 BC emissions (Gg/yr/grid) along with percent change (w.r.t to base year 2005) in (b) Reference 2030 BC emissions c) 2030 BC emissions with BC measures (low) and d) 2030 BC emissions with BC (lowest) and greenhouse gas measures aimed at keeping CO_2 levels below 450ppm. The triangle and circle markers denote locations of the LST and Bishkek sites. Refer to Sec. 2.3 for more details on emission scenarios.

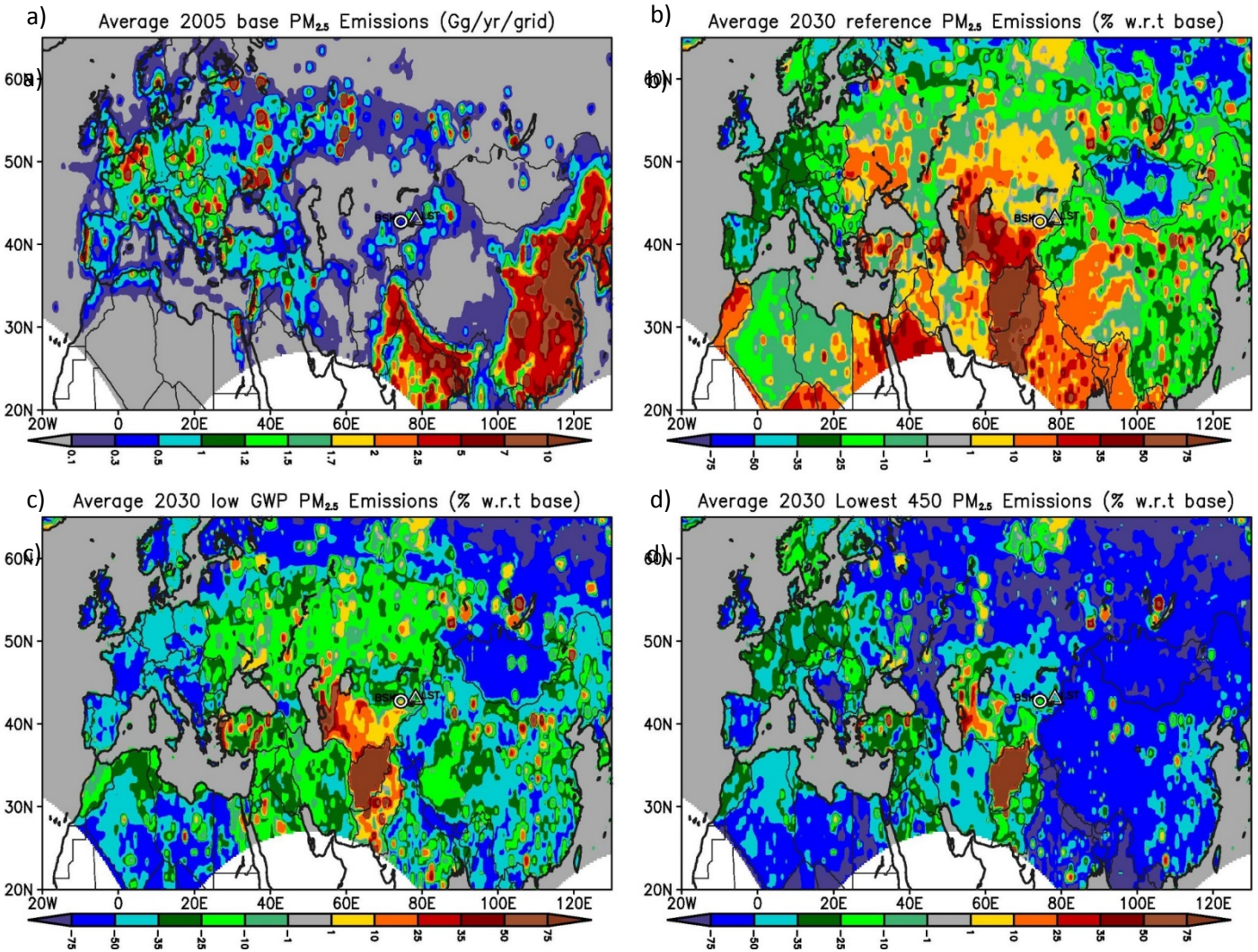

Fig. S3. Spatial distribution of a) base year 2005 $PM_{2.5}$ emissions (Gg/yr/grid) along with percent change (w.r.t to base year 2005) in (b) Reference 2030 $PM_{2.5}$ emissions c) 2030 $PM_{2.5}$ emissions with BC measures and d) 2030 $PM_{2.5}$ emissions with BC and greenhouse gas measures aimed at keeping CO_2 levels below 450ppm. The triangle and circle markers denote locations of the LST and Bishkek sites. Refer to Sec. 2.3 for more details on emission scenarios.

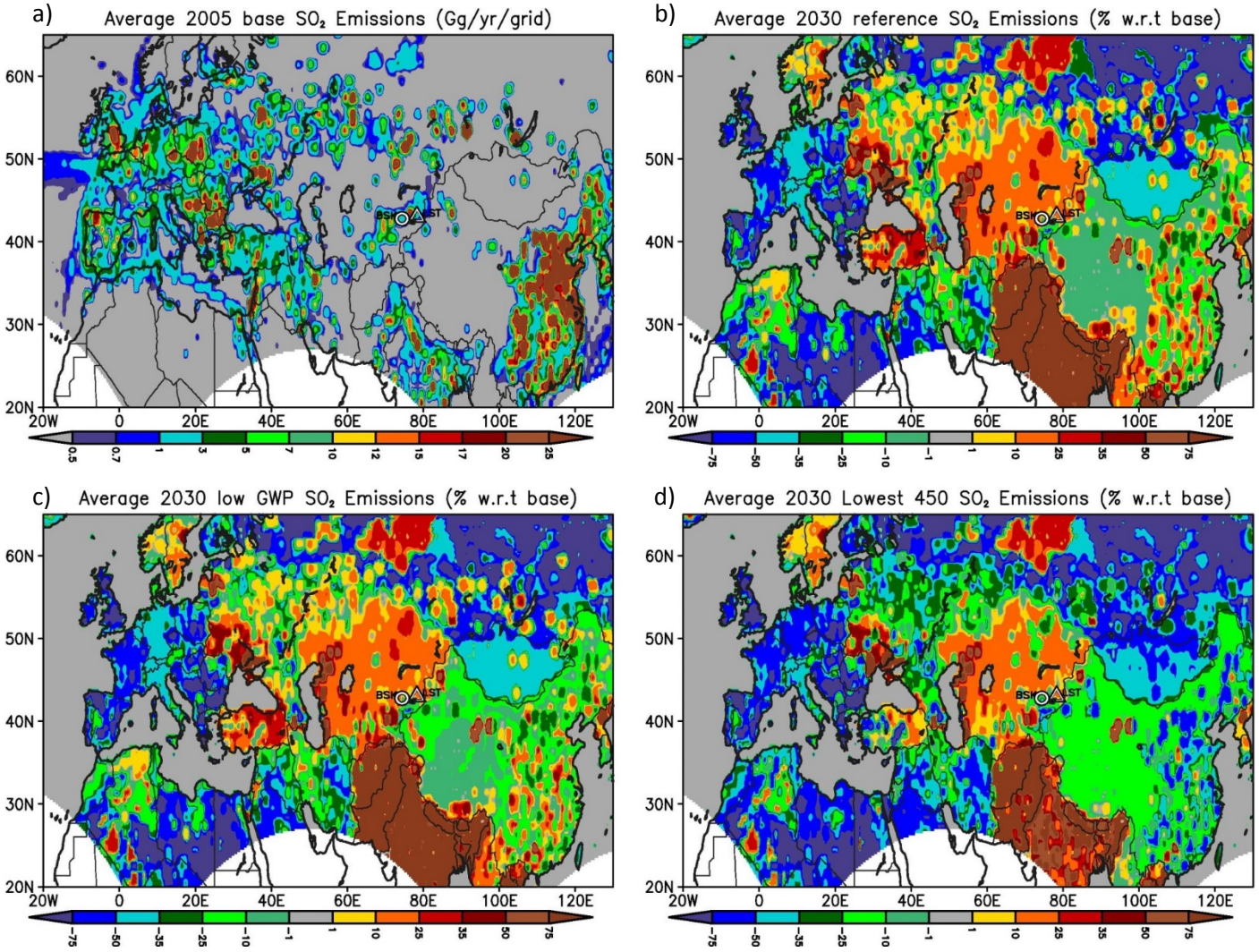

Fig. S4. Spatial distribution of a) base year 2005 SO_2 emissions (Gg/yr/grid) along with percent change (w.r.t to base year 2005) in (b) Reference 2030 SO_2 emissions c) 2030 SO_2 emissions with BC measures and d) 2030 SO_2 emissions with BC and greenhouse gas measures aimed at keeping CO_2 levels below 450ppm. The triangle and circle markers denote locations of the LST and Bishkek sites. Refer to Sec. 2.3 for more details on emission scenarios.

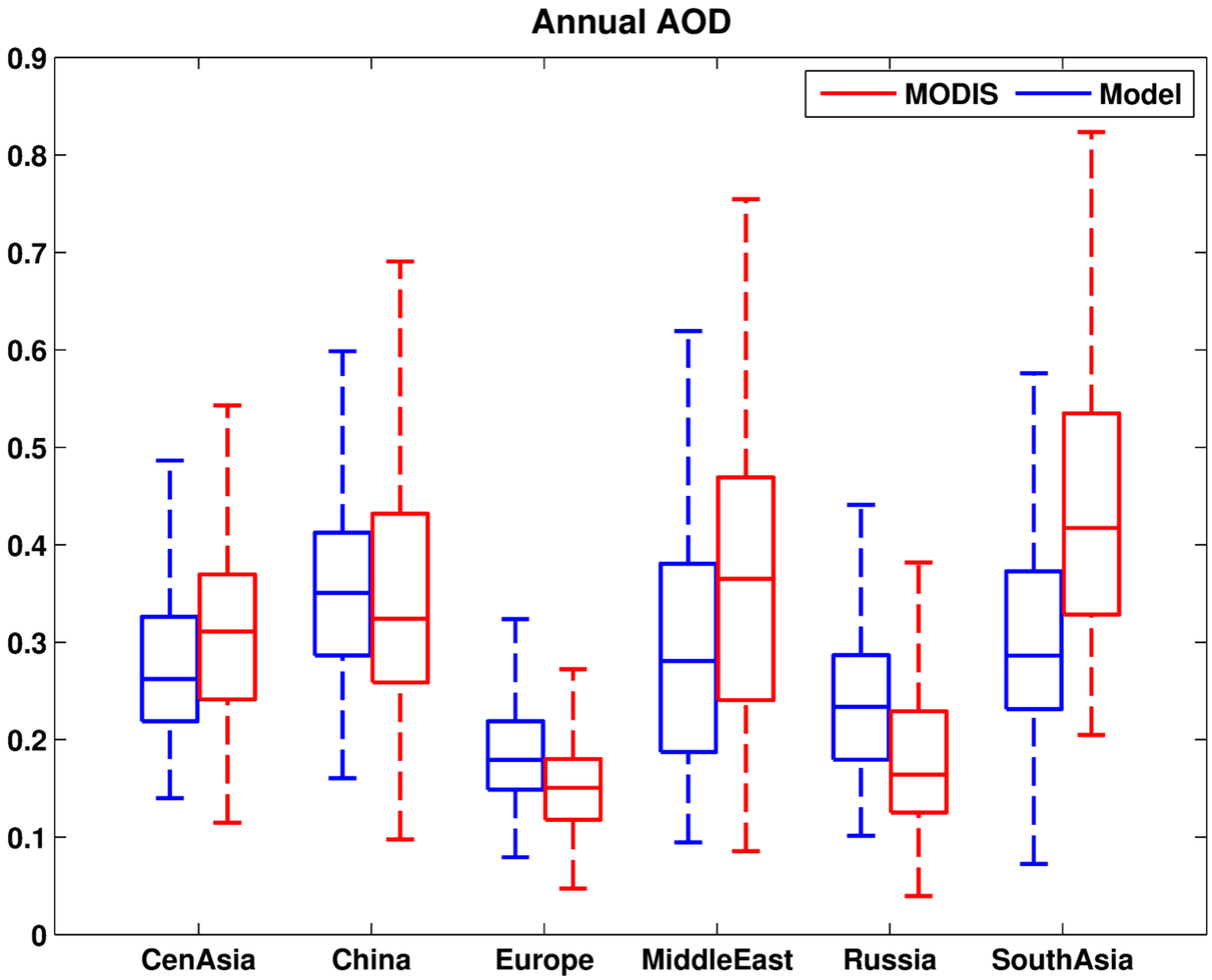

Fig. S5. Comparison of regional average AOD from MODIS with simulated AOD shown as box plots over the simulation period for selected source regions including Central Asia, China, Europe, Middle East, Russia and South Asia. (See Fig 1 and Sect.3.2 for more details)

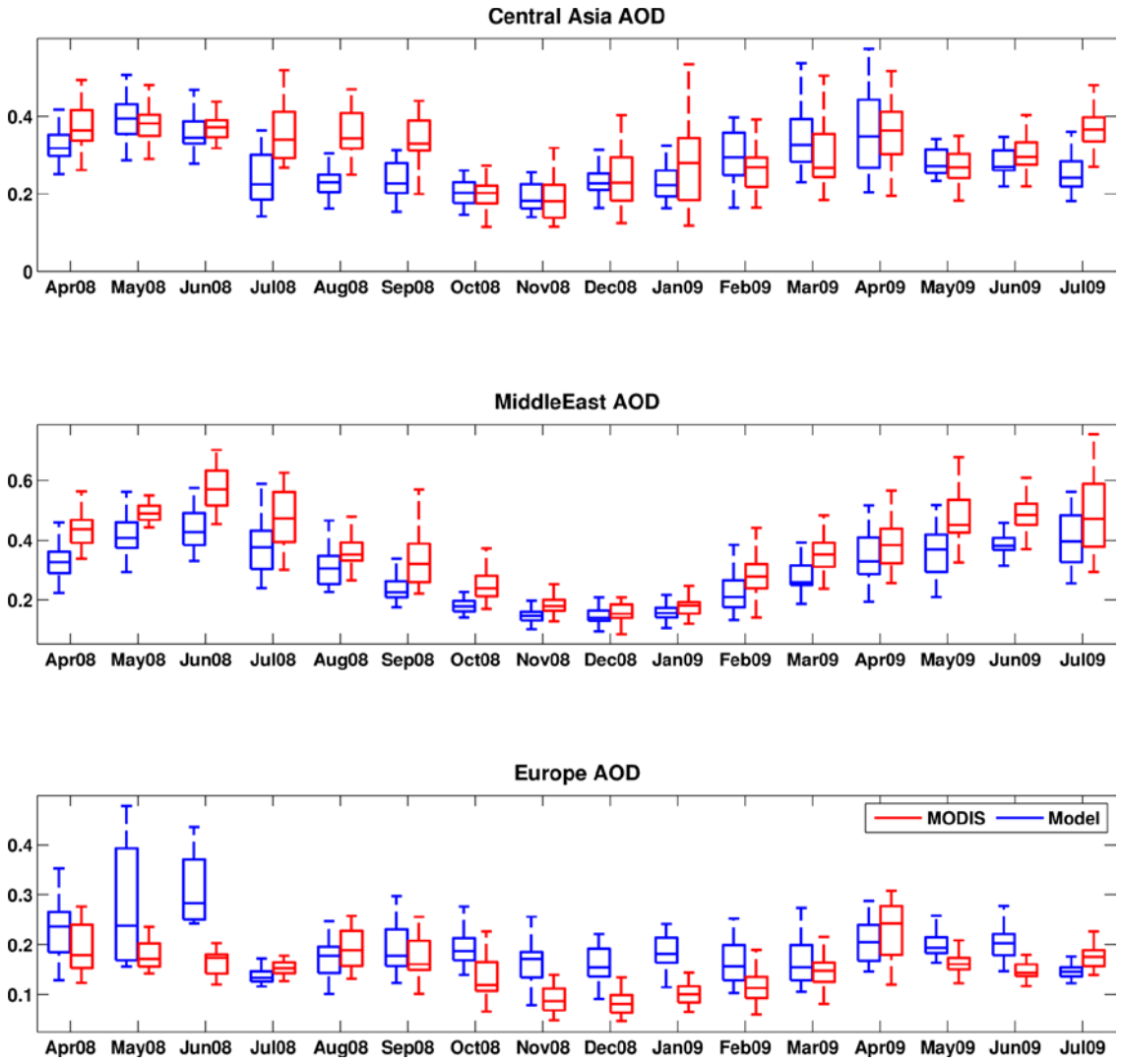

Fig. S6. Comparison of regional average AOD from MODIS with simulated values shown as monthly box plots over the simulation period for selected source regions (a) Central Asia (b) Middle East and (c) Europe (See Fig 1 and Sect.3.2 for more details)

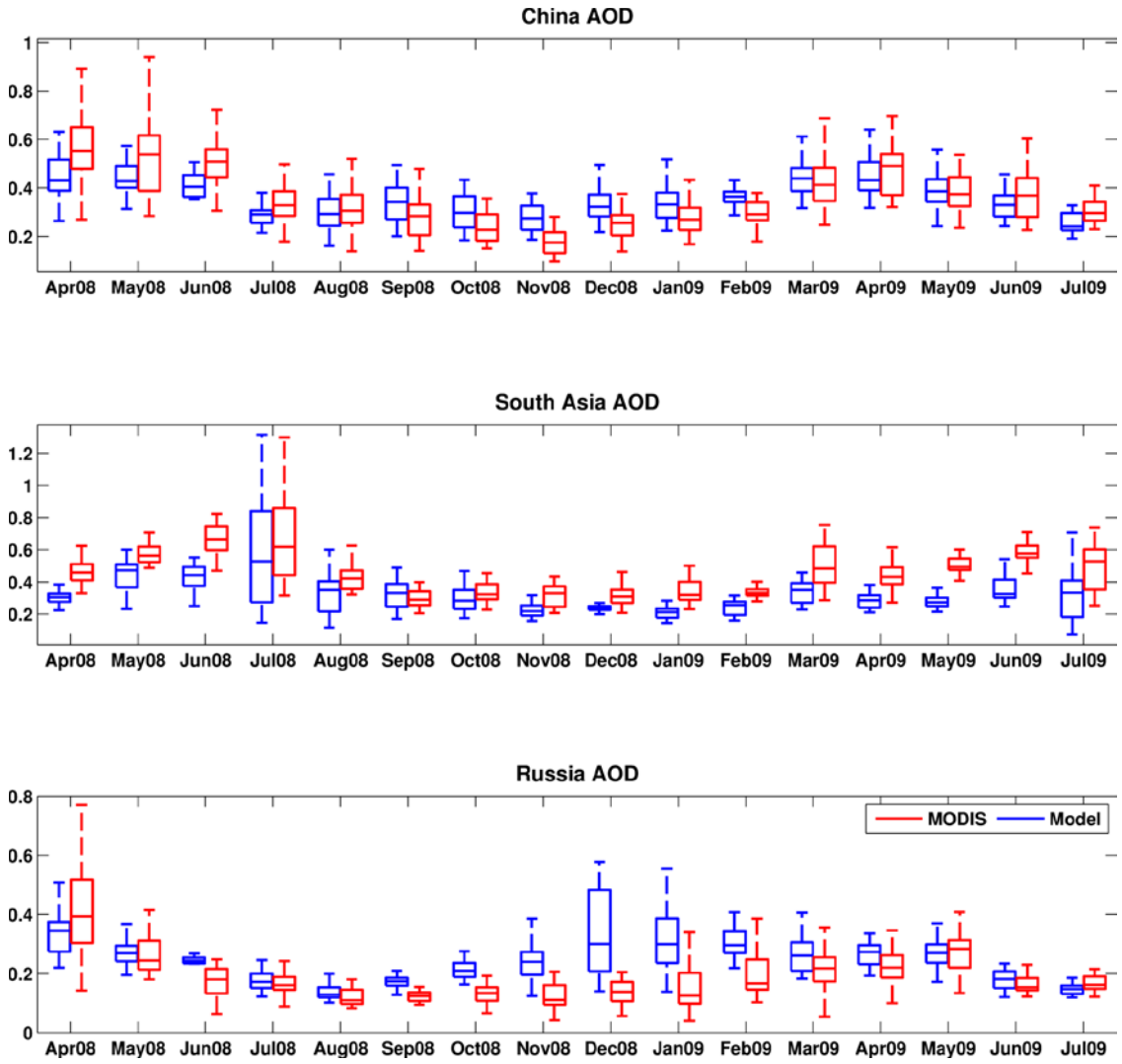

Fig. S6….. continued. Comparison of regional average AOD from MODIS with simulated values shown as monthly box plots over the simulation period for selected source regions (d) China, (e) South Asia and (f) Russia (See Fig 1 and Sect.3.2 for more details)

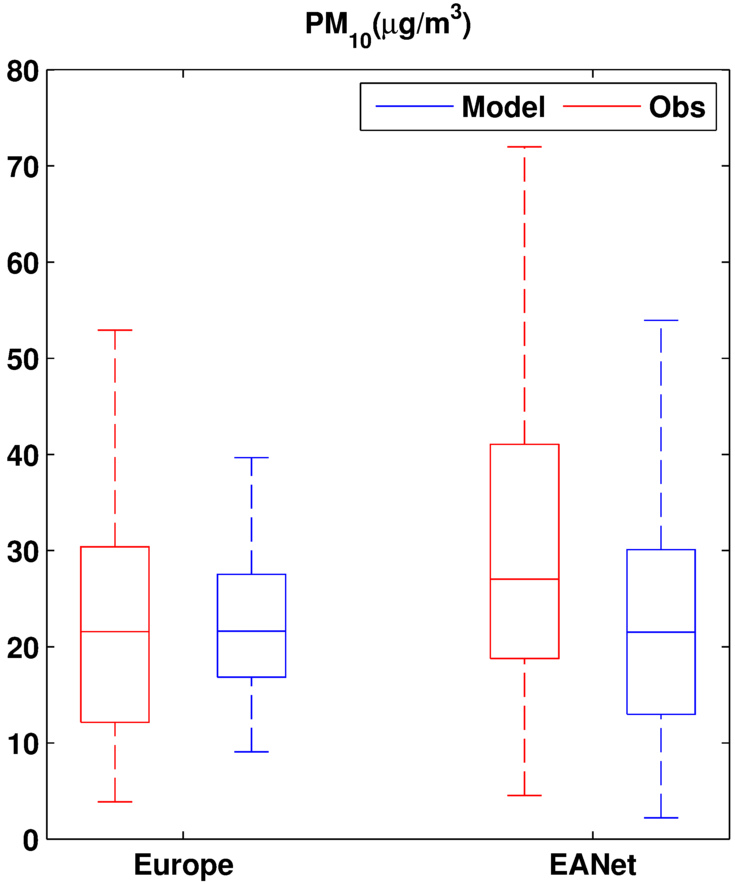

Fig. S7. Comparison of predict PM_{10} with monthly observations from the European Monitoring and Evaluation Programme (EMEP available at http://www.nilu.no/projects/ccc/emepdata.html) and the Acid Deposition Monitoring Network in East Asia (EANET available at http://www.eanet.asia/product/index.html) surface site networks shown as box and whisker plots over the simulation period In each box whisker panel, the middle line denotes the median value, while the edges of the box represent 25th and 75th percentile values respectively. The whiskers denote the maximum and minimum values.

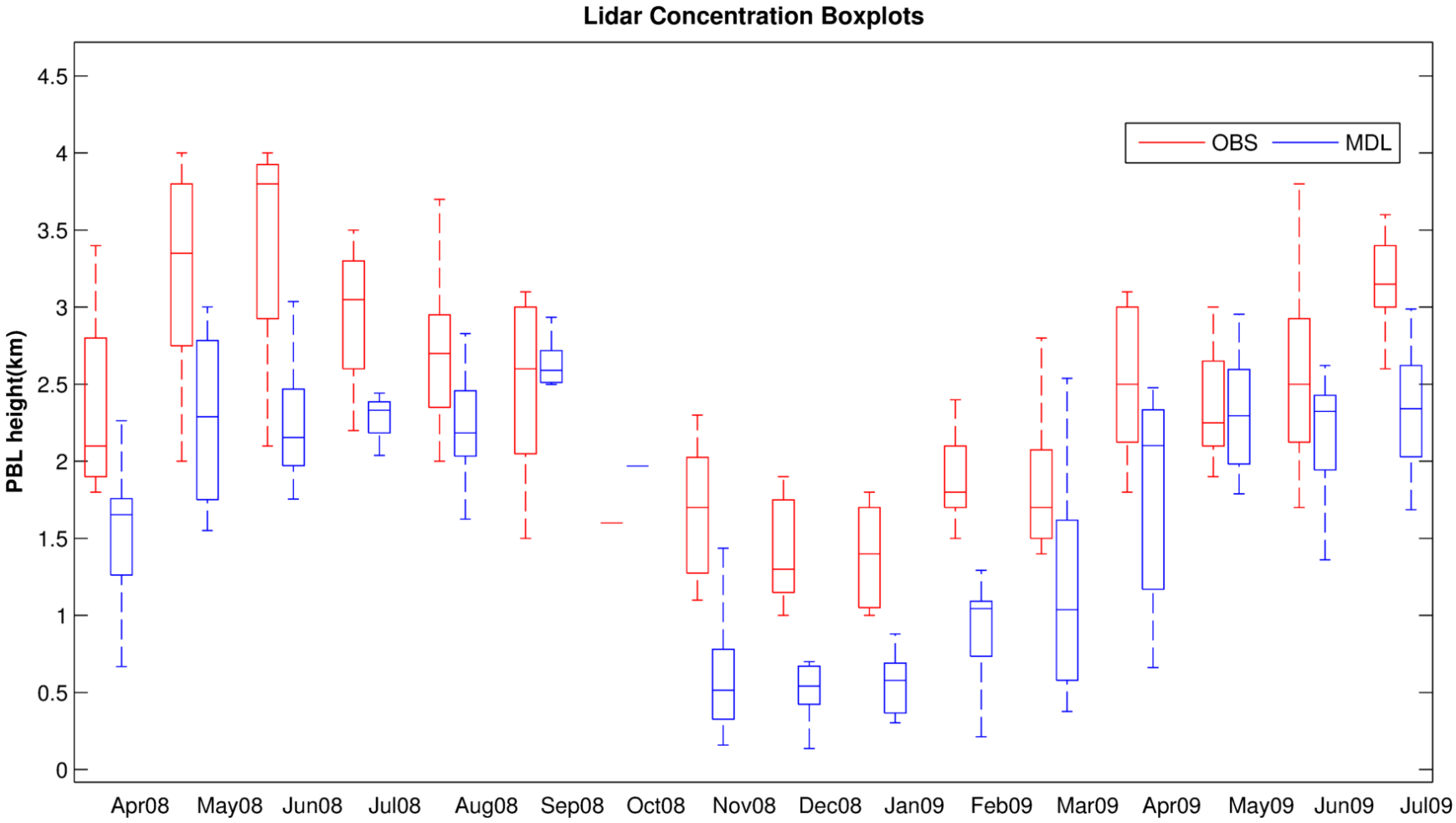

Fig. S8. Comparison of observed and predicted PBL heights (m) at the LST site. Observed PBL heights were determined from the Lidar profiles.

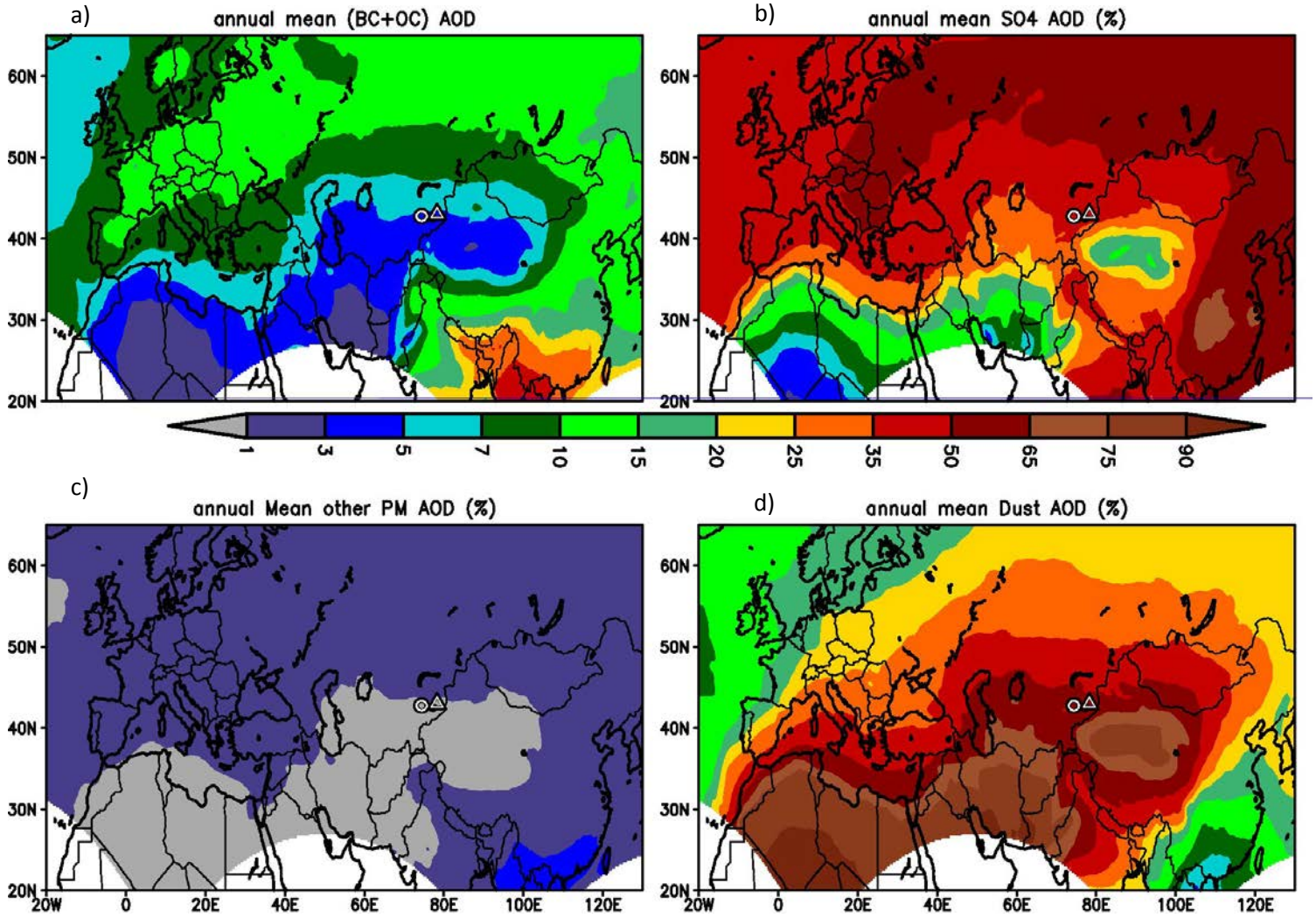

Fig. S9. Spatial distribution of predicted species contributions (%) to AOD averaged over the simulation period a) Carbonaceous aerosols (BC+OC), b) SO4, c) Other PM, and d) Dust.

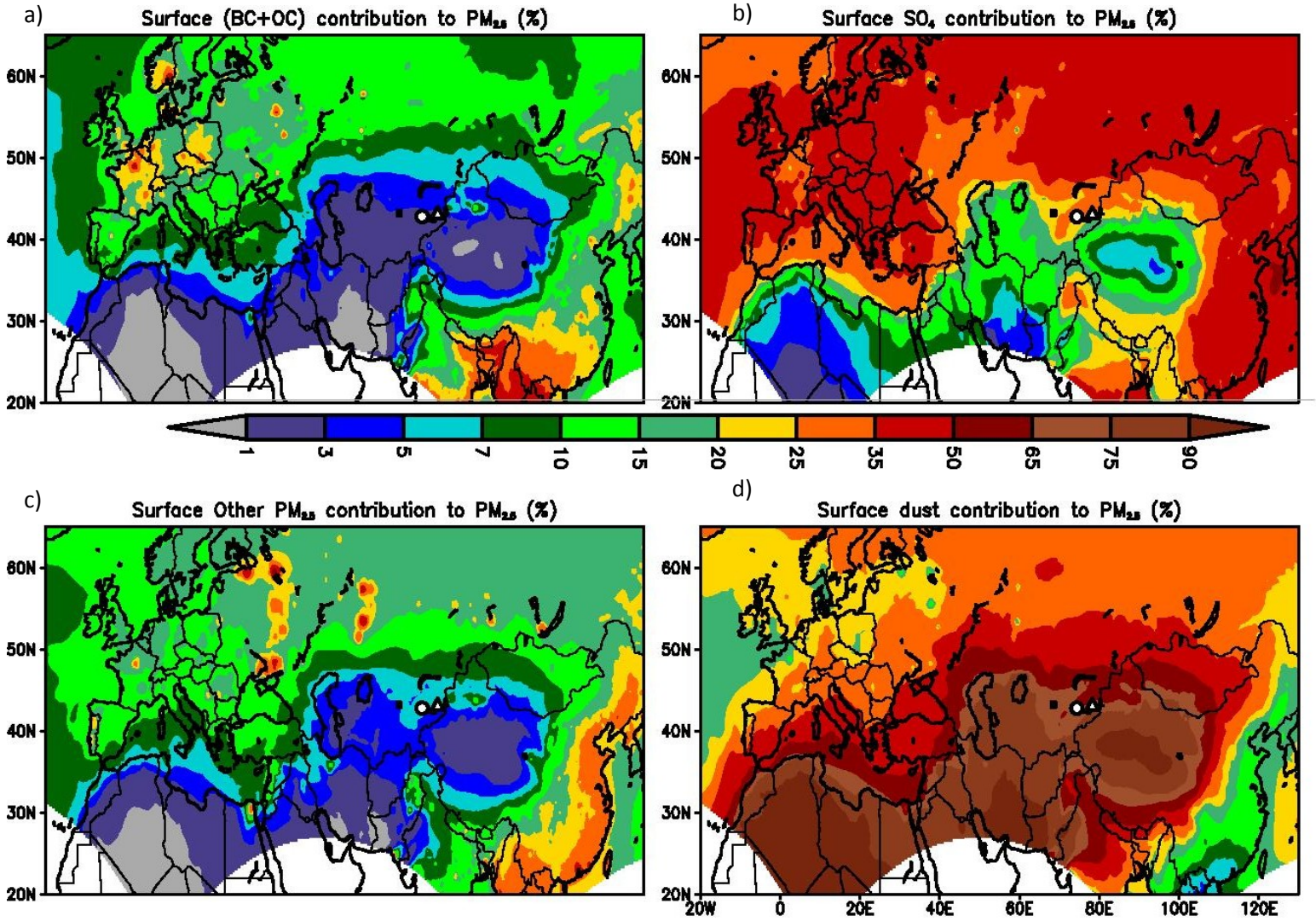

Fig. S10. Spatial distribution of predicted species contributions (%) to $PM_{2.5}$ averaged over the simulation period a) Carbonaceous aerosols (BC+OC), b) SO4, c) Other $PM_{2.5}$, and d) Dust.

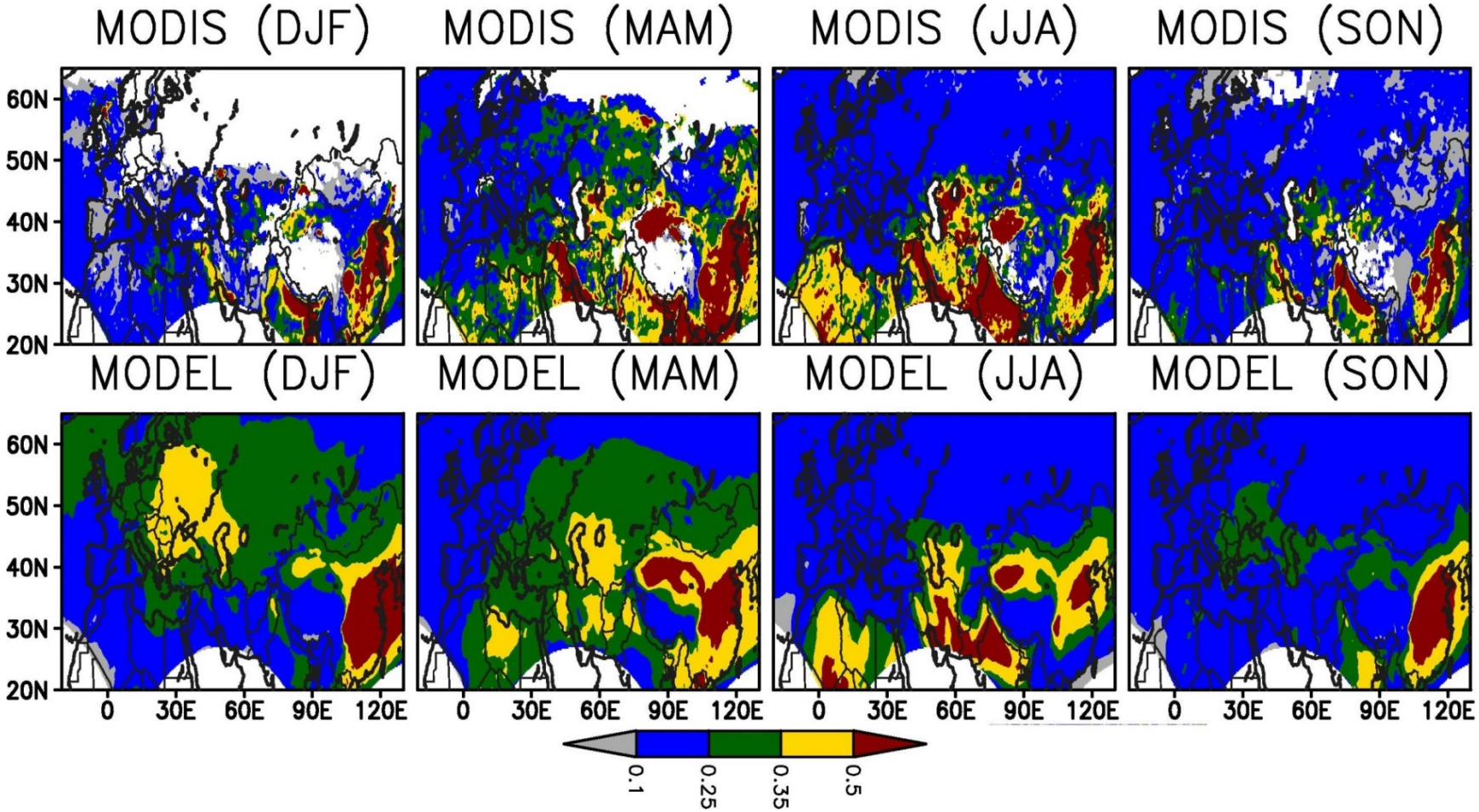

Fig. S11 Seasonal variability in spatial distribution of MODIS and simulated AOD averaged over the simulation period.

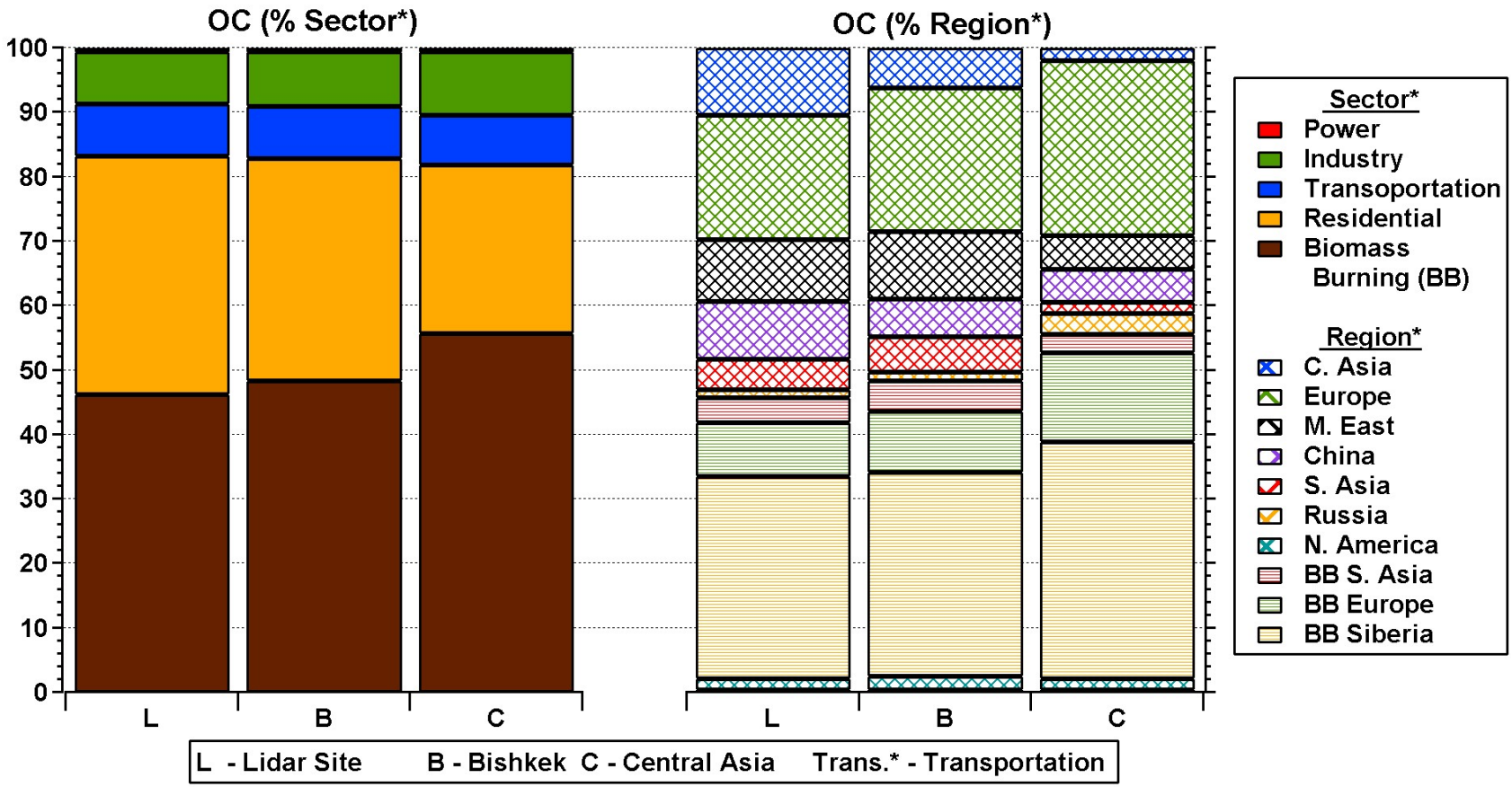

Fig S12. Summary of period mean contributions by source regions and sectors for OC in % for the grid cells containing the Bishkek and LST observation sites, and spatially averaged over the Central Asia region. See Fig. 1 for anthropogenic and fire source regions.